International Journal of Biological Macromolecules 68 (2014) 241–246

Contents lists available at ScienceDirect

International Journal of Biological Macromolecules

journal homepage: www.elsevier.com/locate/ijbiomac

Gellan co-polysaccharide micellar solution of budesonide for allergic anti-rhinitis: An *in vitro* appraisal

Sabyasachi Maiti*, Amrita Chakravorty, Moumita Chowdhury

Department of Pharmaceutics, Gupta College of Technological Sciences, Ashram More, G.T. Road, Asansol 713301, West Bengal, India

ARTICLE INFO

Article history:
Received 8 March 2014
Received in revised form 28 April 2014
Accepted 4 May 2014
Available online 10 May 2014

Keywords:
Gellan polysaccharide
Sorbitan monooleate
Budesonide
Dissolution efficiency
Polysaccharide micelles
Anti-rhinitis

ABSTRACT

The aim of this study was to design a novel amphiphilic co-polysaccharide for the development of anti-rhinitis micellar solution of budesonide. Herein, a long alkyl chain (C_{18}) was successfully grafted onto gellan polysaccharide by etherification reaction. The dispersion of co-polysaccharide in water led to formation of spherical, nanomicellar structures. Depending upon the co-polysaccharide:drug weight ratio (1:1, 1:2 and 1:3), a maximum drug loading (>95%) was noted at the lowest level. The nanomicelles were in the range of 371–750 nm and showed negative zeta potential (−48.3 to −67.2 mV) values indicating their stability in aqueous system. They exhibited a longer dissolution profile in simulated nasal fluid (pH 5.5). The dissolution efficiency (39.79 ± 0.93%) was maximal at the lowest polymer: drug ratio in 6 h. The drug release was found to follow first order kinetic model. Korsmeyer-peppas modeling of *in vitro* drug release data indicated that besides simple diffusion, no other physical phenomenon was involved in the event of drug release from the nanostructures. Differential scanning calorimetry analysis suggested some degree of physical incompatibility; however Infrared spectroscopy revealed chemical compatibility between drug and co-polysaccharide. Thus, the co-polysaccharide micellar system offers a splendid outlook in controlled intranasal delivery of budesonide for the symptomatic relief of anti-rhinitis.

1. Introduction

About 40% of potentially valuable drug candidates identified by high throughput screening are rejected and never enter a formulation development stage due to their poor water solubility [1]. In particular, the development of liquid formulation offers a challenge to pharmaceutical scientists.

To minimize drug degradation, loss upon administration, prevent harmful or undesirable side-effects, various drug delivery systems are currently being developed or under development [2]. In modern pharmaceutics, intranasal delivery is considered as a route of choice for local effect rather than systemic effect. Delivery of drugs *via* nose for maintenance therapy of nasal allergy, sinusitis, nasal congestion, and nasal infections is a routine practice [3].

To enhance water solubility of some drugs, certain clinically acceptable organic solvents are used in their formulations. Alternatively, certain micelle-forming surfactants have been used in formulations of insoluble drugs. The administration of many co-solvents or surfactants causes toxicity and other undesirable side effects [4]. The use of liposomes and β-cyclodextrins demonstrated some promising results with certain poorly soluble drugs, although the solubilization capacity of the liposomal membrane and cyclodextrin inner cavity for water-insoluble molecules is rather limited [5]. Surfactants cannot retain solubilized material at concentrations lower than their critical micelle concentration (CMC), which is typically rather high in cases of conventional low molecular weight surfactants [6]. Possible precipitation upon dilution of the drug solutions in water–organic solvent mixtures depends on a variety of factors and must be investigated for each excepient–drug combination of interest. Thus, the solubilization of poorly water soluble drugs still remains an important concern.

Intranasal delivery of drugs is the natural choice for topical treatment of local diseases in the nose and paranasal sinuses such as allergic and non-allergic rhinitis and sinusitis [7]. The benefit of using drugs in a nasal spray is that it is delivered immediately to the site of nasal allergy symptoms—inside the nose. In these cases, intranasal route is the primary option for drug delivery because it allows a rapid symptomatic relief with a more favorable adverse-event profile than oral or parenteral routes. In fact, relatively low doses are effective when administered topically; minimizing simultaneous potential of systemic toxic effects [8].

Budesonide is an anti-inflammatory synthetic corticosteroid and is designated chemically as (11β, 16α)-16,17-[butylidene *bis*(oxy)]-11, 21-dihydroxypregna-1,4-diene-3,20-dione. It is

* Corresponding author. Tel.: +91 9474119931; fax: +91 341 2314604.
E-mail address: sabya245@rediffmail.com (S. Maiti).

http://dx.doi.org/10.1016/j.ijbiomac.2014.05.003
0141-8130/

administered via nasal route as spray or drops to decrease inflammation in the nasal passages. Nasal inflammation occurs when the nasal passages are exposed to foreign particles like pollen, dust mites or pet fur. The allergens cause the cells in the nose to release chemicals that produce immune and allergic responses. People who suffer from allergic rhinitis tend to experience a variety of symptoms which include a runny, itchy or blocked nose, sneezing and sinus discomfort [9]. Following intranasal administration, budesonide is absorbed into the affected tissues/cells of the nasal passages and prevent these cells from releasing the chemicals. This stops the allergic reaction from happening, so the nasal inflammation is reduced and the symptoms relieved [10].

Most manufacturers recommend their product for use twice daily, less if warranted. However, they take several days to act and hence, need to be taken continually for several weeks as their therapeutic effect builds up with time. The frequent and long-term use is known to cause a dependency to the medications used in many over the counter sprays. This can lead to damage to the sensitive membranes in the nose, and eventually leads to rupture and frequent nosebleeds. In addition, frequent nasal spray use can have the opposite effect of what the medication is meant to do. Membranes may become so irritated and inflamed, nasal passages are not clear unless nasal spray is administered.

Recently, the use of amphiphilic copolymer has drawn much attention for the solubilization and development of poorly soluble drugs. The amphiphiles are so designed that they can form nanomicellar (core and shell) structures in water, wherein the inner hydrophobic core encapsulates the poorly water-soluble drugs, and the outer hydrophilic shell protects the drug from aqueous environment [11,12]. Now, the drug is well protected from possible inactivation under the effect of biological surroundings and prevents the exposure of a local, high drug concentration on tissues, thus minimizing tissue irritation.

In most cases, the hydrophilic outer shell consists of poly(ethylene oxide) (PEO) chains, owing to their high degree of hydration. To build hydrophobic core-forming blocks, a variety of polymers have been investigated and these include poly(propylene oxide) [13], poly(L-lysine) [14], poly(aspartic acid) [15], poly(ε-caprolactone) [16], and poly(D,L-lactic acid) [17].

Because of their biocompatibility, biodegradability, and the multiplicity of functional groups for the conjugation of pilot molecules [18], polysaccharides have now become the polymer of interest as hydrophilic segment of the copolymer. However, the reports on polysaccharide-based micellar systems are scarce in the literature. Notable examples of the co-polysaccharides include dextran- or hydroxypropylcellulose-*g*-PEO_{10}-C_{16} [19], N-palmitoyl chitosan [20], stearyl chitosan and sulfated stearyl chitosan [21], methoxy poly(ethylene glycol)-*g*-chitosan [22].

Gellan is an anionic, hydrophilic bacterial exo-polysaccharide which consists of repeating tetrasaccharide units of β-D-glucose, β-D-glucuronic acid, and α-L-rhamnose residues [23]. No reports are available so far that describes the use of gellan polysaccharide as a hydrophilic shell for the design of amphiphilic copolymer. Thus, the objective of this present investigation is to synthesize a novel, amphiphilic gellan co-polysaccharide for intranasal delivery of budesonide.

2. Materials and methods

2.1. Materials

Budesonide was a gift from Sun Pharma Advance Research Company Ltd., Gujarat, India. Gellan gum was purchased from SRL Pvt. Ltd., Mumbai, India. Sorbitan monooleate was supplied by Loba Chemie Pvt. Ltd., Mumbai, India. Thionyl chloride ($SOCl_2$) and dimethylsulfoxide (DMSO) was procured from Merck Specialities Pvt. Ltd., Mumbai, India. All other analytical reagents were used as received from the suppliers.

2.2. Synthesis of C_{18}-g-gellan co-polysaccharide

The synthetic procedure was described as follows. Initially, 20 ml of thionyl chloride was added to 5% (w/v) solution of sorbitan monooleate in chloroform and refluxed for 2 h without heat for chlorination. A semisolid, blackish brown mass of chlorinated sorbitan monooleate was obtained.

Later, a homogenous dispersion of gellan polysaccharide (3%, w/v) was prepared in dimethyl formamide (DMF) and the temperature of the dispersion was maintained at 10 °C. To this, same amount of sodium hydride was added. After this, a dispersion of chlorinated sorbitan monooleate in DMF (0.02%, w/v) was also added. Thereafter, the resultant mixture was stirred for 1 h at room temperature and the total reaction mixture was transferred into 50 ml of distilled water. Subsequently, the co-polysaccharide layer was isolated and adjusted to pH 7.0. The co-polysaccharide was purified in ethanol, filtered off and air-dried.

2.3. Fourier Transform Infrared (FTIR) spectroscopy

FTIR spectra of gellan polysaccharide, co-polysaccharide and sorbitan monooleate were recorded over the range of 4000–400 cm^{-1} wave numbers using KBr pellets (Perkin-Elmer, Spectrum RX1, UK). To ascertain co-polysaccharide–drug interaction, infrared spectra of pure drug and drug-loaded co-polysaccharide were also recorded.

2.4. Morphology of co-polysaccharide micelles

The co-polysaccharide was dispersed in double distilled water and a drop of solution was put onto microscopic slide. The slide was observed under an optical microscope, fitted with a digital camera Moticam 1000 (1.3 mega pixel) at 40× magnification (Magnus MLX, Olympus, India). The morphological structures were captured using Motic Images Plus 2.0 software.

2.5. Preparation of drug-loaded co-polysaccharide micelles

The loading of budesonide into co-polysaccharide micelles was accomplished by solvent evaporation method. A known amount of the co-polysaccharide (100 mg) was dispersed into 100 ml of water under magnetic agitation. Subsequent to this, budesonide dissolved in 50 ml of ethanol was added gradually and stirred for 4 h. The resulting solution was probe-sonicated for additional 2 h. Finally, the solution was filtered through Whatman filter paper no. 1 (pore size 11 μm) and the filtrate was freeze-dried. The co-polysaccharide: drug weight ratio was varied (1:1, 1:2 and 1:3) and three different micellar formulations were prepared. Drug-free formulation was also prepared by the same method without the use of ethanol.

2.6. Determination of drug entrapment efficiency

Accurately weighed, 10 mg of freeze-dried product was dissolved in 10 ml DMSO and the absorbance of the resulting solutions was measured with a spectrophotometer (UV1, Thermo Spectronic, UK) at 281 nm using co-polysaccharide solution in DMSO (1 mg/ml) as blank. All samples were analyzed in triplicate. The drug entrapment efficiency was calculated by the following equation:

$$\text{DEE}\,(\%) = \frac{\text{actual drug content}}{\text{theoretical drug content}} \times 100$$

The reliability of this method was assessed through recovery analysis. Here, a known amount of drug was analyzed spectrophotometrically both in presence and absence of co-polysaccharide. The actual drug estimated analytically was expressed as a percentage recovery and the recovery averaged 98.89 ± 0.04% for the three determinations.

2.7. Size and zeta potential

The size and zeta potential of the co-polysaccharide micellar systems were measured were by Malvern zetasizer Ver. 6.00 apparatus (Malvern Instruments Ltd., Worcestershire, UK) at 25 °C.

2.8. Differential scanning calorimetry (DSC)

The samples of pure drug, drug-loaded and drug-free co-polysaccharide micelles were analysed for their typical thermograms (PerkinElmer, Pyris Diamond TG/DTA, Osaka, Japan). Each sample (2–6 mg) was hermetically sealed into an aluminium pan and was heated at a rate of 10 °C/min. The thermograms were traced under nitrogen flow (20 ml/min) over 100–300 °C. Platinum crucible with alpha aluminium powder was used as reference for the calibration of the instrument.

2.9. In vitro drug release

Simulated nasal fluid (SNF, pH5.5) was prepared by dissolving 8.77 g NaCl, 2.98 g KCl and 0.59 g $CaCl_2$ in 1 l of water. Each freeze-dried products (10 mg) were dispersed in 5 ml SNF and placed in HiMedia dialysis tube (average flat width 39.41 mm; average diameter 23.8 mm; capacity 4.45 ml/cm, MWCO 12–14 kDa). The dialysis bag was tied and dialysed against 50 ml of SNF. The fluid in receptor compartment was magnetically stirred at 150 rpm and the temperature was maintained at 37 ± 1 °C. One millilitre of aliquot was withdrawn from the receptor compartment at specified time intervals and immediately replenished with the same volume of fresh fluid. The samples were analyzed at 246 nm without filtration and further dilution (UV1, Thermo Spectronic, UK). Cumulative percentage of drug released in SNF was plotted as a function of time. Each sample was analyzed in triplet.

2.10. Data treatment

The area under curve of the drug release profiles were calculated by GraphPad Prism Version 5.00 (Trial) software and used for the determination of dissolution efficiency of micellar solutions. The differences in drug entrapment and dissolution efficiencies of the solutions were analysed by one way analysis of variance (ANOVA): single factor using Microsoft Excel 2002 software. The difference was considered significant when $p < 0.05$.

3. Results and discussion

3.1. Characterization of co-polysaccharide

The nonspecific chlorination of sorbitol hydroxyl groups of sorbitan monooleate was conducted in presence of thionyl chloride. The by-products of this conversion were hydrochloric acid (HCl) and sulphur dioxide (SO_2) which easily bubbled away and no further purification step is required for the chlorinated samples. The chlorination of sorbitan monooleate was confirmed by qualitative Beilstein test. Herein, the tip of a copper wire was heated in a burner flame until there was no further coloration of the flame. Then, the wire was cooled slightly, and dipped into the chlorinated sample. As the wire heated, a green flash was observed, indicative of

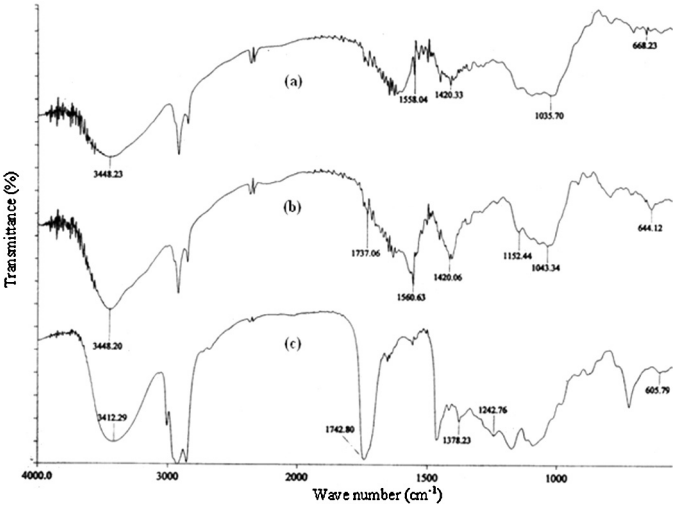

Fig. 1. FTIR spectra of (a) gellan polysaccharide; (b) C_{18}-*g*-gellan co-polysaccharide; and (c) sorbitan monooleate.

chloride ion in the sample. The addition of sodium hydride to gellan polysaccharide dispersion led to the formation of reactive alkoxide ($-O^-Na^+$). Further reaction with chlorinated samples gave birth to ether linkages. The reaction scheme can be described as follows.

$$C_{17}H_{33}COOC_6H_{13}O_5(\text{Sorbitan Monooleate}) + SOCl_2 = C_{17}H_{33}COOC_6H_{12}O_4Cl + SO_2 + HCl \quad \text{(i)}$$

$$\text{Gellan–OH} + NaH \rightarrow \text{Gellan–ONa} \quad \text{(ii)}$$

$$(C_{17}H_{33}COOC_6H_{12}O_4)Cl + \text{Gellan–ONa (Alkoxide)} = \text{Gellan–O–}O_4H_{12}C_6OOCH_{33}C_{17}\text{(Gellan Copolymer)} + NaCl \quad \text{(iii)}$$

In FTIR spectrum of gellan polysaccharide, the C=O stretching vibrations of carboxylate anion were observed at frequencies of 1420.33 cm^{-1} (symmetric) and 1558.04 cm^{-1} (asymmetric) (Fig. 1a).

In the copolymer, the C=O stretching vibrations of carboxylate anion were also found at 1420.06 cm^{-1} (symmetric) and 1560.63 cm^{-1} (asymmetric) [24]. This suggested that COO^- anion remain un-reacted during chemical modifications. In gellan polysaccharide, a sharp band appeared at 1035.70 cm^{-1} and this was attributed to C–O stretching of C–OH groups in carbohydrates. The same stretching vibration appeared in the spectrum of co-polysaccharide at 1043.34 cm^{-1}. Thus, it was quite reasonable that all the hydroxyl groups of gellan polysaccharide did not react with the hydrophobic moiety (C_{18}) to produce the co-polysaccharide. A broad O–H stretching centred on 3448.23 cm^{-1} was noted in the spectrum of native gellan. The O–H stretching was also evident at 3448.20 cm^{-1} in the co-polysaccharide. A sharp, intense C=O stretching band of sorbitan esters was evident at 1742.80 cm^{-1} in the spectrum of sorbitan monooleate (Fig. 1c). The band at 1378.23 cm^{-1} was also assigned to the C–O stretching of esters [25]. A very weak C=O stretching of ester groups was visible in the spectrum of the co-polysaccharide at 1737.06 cm^{-1} and this could be due to presence of bulkier chain in the co-polysaccharide. A new band appeared at wave number 1152.44 cm^{-1} was due to C–O stretching of ethers (Fig. 1b). This confirmed the synthesis of co-polysaccharide.

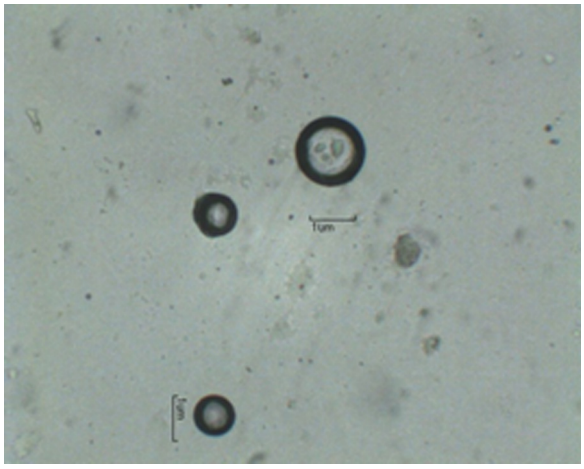

Fig. 2. Morphological structures of C_{18}-*g*-gellan co-polysaccharide micelles.

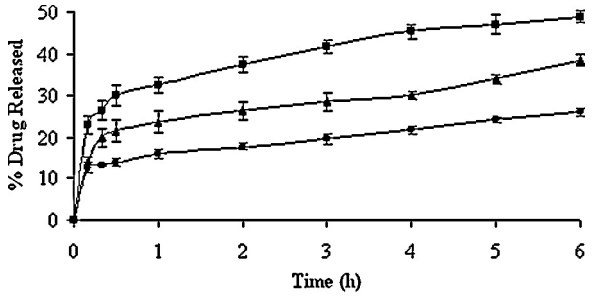

Fig. 3. *In vitro* drug release profiles of the co-polysaccharide micelles in pH 5.5 SNF. Key: (■) A; (▲) B; (●) C.

3.2. Properties of co-polysaccharide

As a known amount of co-polysaccharide was dispersed in water under continuous magnetic agitation, it gradually disappeared. Microscopic examinations revealed that the co-polysaccharide formed spherical nanostructures, which was termed 'co-polysaccharide micelles' (Fig. 2). Because it associated in water and assumed core-shell nanostructures, the co-polysaccharide was said to have amphiphilic property.

Preliminary investigation suggested that the co-polysaccharide could form micellar structures even at concentration range of 0.25–0.5 mg/ml but the micelles could not hold a reasonable amount of drug. Microscopic study confirmed the existence of micelles at these concentrations. However, the micelles entrapped almost the entire drug at 1 mg/ml concentration of the co-polysaccharide. Hence, it was decided to design micellar formulations keeping the co-polysaccharide concentration constant at 1 mg/ml.

To understand the properties of co-polysaccharide micelles, the co-polysaccharide: drug weight ratio was varied (1:1, 1:2 and 1:3). Budesonide was incorporated into the micellar structures by solvent evaporation method. It became very difficult to differentiate between the drug-loaded and drug-free nanomicellar structures. Hence, only a representative photograph was cited herein (Fig. 2). The yield of micellar product gradually decreased with increasing weight ratio and was about 62–84%. Similar trend was noted in their *z*-average diameter which ranged between 371 and 750 nm (Table 1). Polydispersity index is a parameter that defines the particle size distribution. Samples with very broad size distribution have polydispersity index values greater than 0.7 [26]. The higher the index, the wider is the size distribution. The data suggested that the co-polysaccharide micelles followed a pattern of narrow size distribution (Table 1). The drug entrapment efficiency of the micelles remained very high (>95%) with the lowest co-polysaccharide: drug ratio (1:1). However, a decreasing tendency was apparent with increasing ratios (45–47%). This magnitude of differences in their drug entrapment efficiency was found statistically significant ($p < 0.05$). To corroborate the results, some useful literature reports were consulted. It was interesting to note that poly(ε-caprolactone)-*g*-dextran copolymer micelles were smaller in diameter and lied in the size range of 80–128 nm [27]. The diameter became much smaller (14–55 nm) in case of copolymer micelles, composed of dextran or hydroxypropylcellulose *grafted* polyoxyethylene cetylether. However, their drug entrapment efficiency was comparatively low (5.5–8.5%) [28]. In a study by Li et al. [29], the smaller diameter of drug-free stearic acid-*g*-chitosan oligosaccharide (CACO) micelles (28.7 ± 18.9 nm) was also reported. However, their size increased to 173.7 ± 37.5 nm after loading of 10-hydroxycamptothecin (HCPT). The HCPT encapsulation efficiency of CACO micelles reached to 76.35% [29]. Although, the gellan co-polysaccharide had comparatively larger particle size but their drug entrapment efficiency was very high and appreciable in comparison to other polysaccharide-based micellar systems available in the art. Nonetheless, the micellar systems based on synthetic hydrophilic polymers reported so far did not show such a higher level of drug entrapment efficiency.

Zeta potential is a measure of the surface charge of dispersed particulate systems and depends on the composition of the particles and the dispersion medium [30,31]. The magnitude of zeta potential is crucial in the stability of the colloidal systems. The dispersions with a large negative or positive zeta potential tend to have better stability against aggregation. Typically, nanoparticles with zeta potential values greater than +25 mV or less than −25 mV have high degree of stability. The dispersions with a low zeta potential value will eventually aggregate due to vander Waal's inter-particle attractions [32]. With the current co-polysaccharide micellar system, zeta potential values were negative and covered a range between −48.3 mV and −67.2 mV (Table 1). As the shell-forming hydrophilic part was made up of negatively charged gellan polysaccharide, the negative zeta potential values could be expected. Moreover, the zeta potential values suggested that the micellar colloidal dispersion was stable in aqueous medium.

In vitro drug release property of these nanomicellar carriers was tested in simulated nasal fluid (SNF, pH 5.5). The drug release profiles were illustrated in Fig. 3.

The micellar carriers having an equal co-polysaccharide: drug ratio liberated only ~50% of the incorporated drug at the end of 6 h and thus exhibited their prolonged drug release potential. The drug release rate became slower as the co-polysaccharide: drug ratio was increased further. Only 26–38% of the incorporated drug

Table 1
Effect of drug: co-polysaccharide weight ratio on the properties of the micelles.

Formulation code	Yield of micelles (%)	*Z*-average diameter (nm)	Polydispersity index	Zeta potential (mV)	Drug entrapment efficiency (%) ± SD, $n = 3$
A	84.12	749.80	0.536	−67.2	95.93 ± 0.41
B	62.31	632.60	0.534	−48.3	47.41 ± 0.22
C	61.89	371.03	0.451	−64.5	45.48 ± 1.35

Table 2
The kinetic rate constants, correlation coefficients and diffusion exponent obtained after fitting *in vitro* drug release data into various kinetic model equations.

Formulation	Zero order		Higuchi model		First order		Korsmeyer-Peppas model		
	r^2	K_0	r^2	K_h	r^2	K_1	n	K_p	r^2
A	0.683	5.549	0.620	23.61	0.965	0.114	0.208	0.3341	0.994
B	0.722	4.231	0.685	16.95	0.905	0.075	0.229	0.2339	0.946
C	0.740	2.922	0.670	11.75	0.882	0.044	0.203	0.1652	0.944

* r^2 indicates correlation coefficient; K_0 (%h^{-1}), K_1 (h^{-1}), K_h (%$h^{-1/2}$), K_p corresponds to zero order, first order, Higuchi and Korsmeyer-Peppas release rate constant, respectively.

released into SNF at higher co-polysaccharide: drug ratio. Later, the dissolution efficiency (DE) of micellar solution was estimated as a function of co-polysaccharide: drug ratio. The dissolution efficiency is defined as the area under dissolution curve up to a certain time, t, expressed as a percentage of the area of the rectangle described by 100% dissolution in the same time [33] and can be represented as follows.

$$\text{Dissolution Efficiency}\,(\%) = \frac{\int_0^t y\,dt}{ty_{100}} \times 100$$

where y is the drug percent dissolved at time t.

The dissolution efficiency of the micelles was ~40% in 6 h at an equal co-polysaccharide: drug ratio (1:1). This value decreased further to ~28% and ~20% at the intermediate and highest ratio, respectively. Following one way ANOVA (single factor), a statistically significant difference was observed between the dissolution efficiency of the micellar solution prepared at three distinct ratios ($p < 0.05$).

In order to assess the kinetics and mechanism of drug release from the nanostructures, *in vitro* drug release data were fitted into various mathematical models: zero order (cumulative % drug release *vs* time), first order (logarithm of % drug remaining to be dissolved), and Higuchi model (% drug release *vs* square root of time) [34,35]. Coefficient of correlation was calculated from the plots using liner regression analyses. The data did not fit at all in zero order and Higuchi kinetic models because the correlation coefficients (r^2) were very poor ($r^2 < 0.740$) (Table 2). Rather, a good linear relationship was observed when the data were fitted into first order kinetic model ($0.882 \leq r^2 \leq 0.965$), which suggested that the drug release was dependent on the amount of drug remaining in the core of the micellar structures. In many systems, the drug release rate is controlled by diffusion and some other physically phenomenon such as swelling or degradation. In order to determine whether a particular device was diffusion-controlled, the early-time release data was fitted into the following empirical relationship [36].

$$\frac{M_t}{M_\infty} = kt^n$$

Usually, the diffusion exponent, n, is dependent on the geometry of the device and the physical mechanism for drug release as well. The systems in which diffusion is the dominant mechanism for drug release is considered as Fickian diffusion ($n \leq 0.43$). The data showed highest correlation when fitted into Korsmeyer-Peppas model ($0.944 \leq r^2 \leq 0.994$). As was evident from Table 2, the value of n was less than 0.43 and hence, Fickian drug transport mechanism was operative *i.e.* the diffusion was driven by chemical potential gradient.

3.3. Drug-co-polysaccharide compatibility

DSC analysis of pure budesonide (Fig. 4a) exhibited a sharp melting endothermic peak at 255.92 °C [37]. In the thermogram of drug-loaded micelles, the characteristics sharp endothermic transition of the drug did not appear at 255.92 °C. Rather, a broad endothermic transition was noted over the temperature range of 200–240 °C (Fig. 4b).

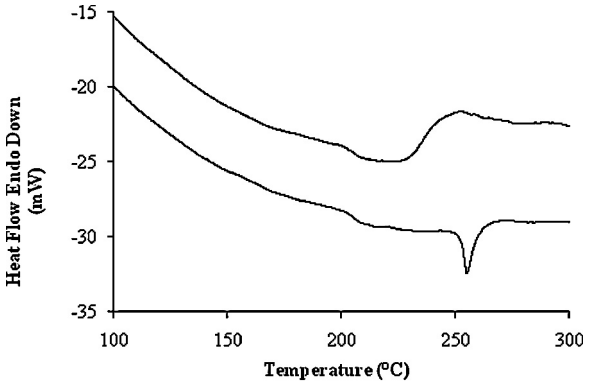

Fig. 4. DSC thermograms of (a) pure budesonide; and (b) budesonide-loaded co-polysaccharide micelles

An endothermic shift towards lower temperature could be due to presence of lipophilic core of the copolymer [38]. The drug-loaded micelles did not reveal complete suppression of the drug's endothermic peak, suggesting a non-homogeneous dissolution of the drug within the co-polysaccharide. Hence, it was inferred that the drug remained mostly in its crystalline state. However, the drug confined in lipophilic micellar core experienced a weak physical interaction.

In FTIR spectrum of pure budesonide (Fig. 5a), the C=O stretching of non-conjugated acetyl and conjugated dihydrobenzoquinone groups was found at 1722.56 cm^{-1} and 1667.06 cm^{-1}, respectively [39].

C–H deformation of $-CH_3$, $-CH_2CH_3$ and $-CH_2CH_2CH_3$ alkyl groups were assigned at 1437.96 cm^{-1}. On the other hand, C–H stretching of alkyl groups and C–O stretching of ketones were evident at 2957.38 cm^{-1} and 1098.79 cm^{-1}, respectively [40]. The

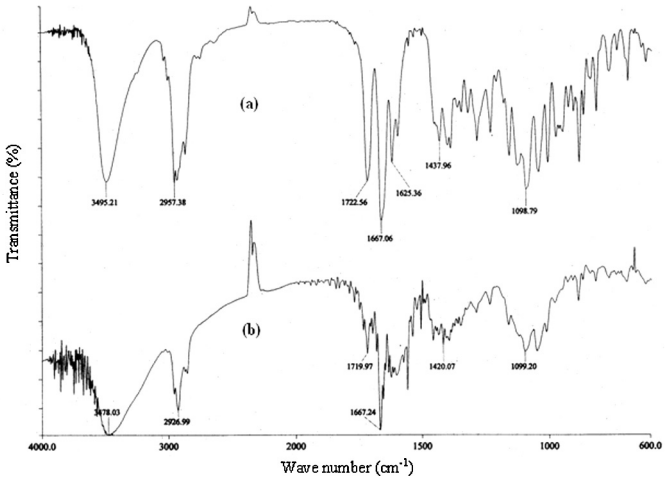

Fig. 5. FTIR spectra of (a) pure budesonide; and (b) budesonide-loaded co-polysaccharide micelles

peak at 3495.21 cm^{-1} could be due to O–H stretching of the hydroxyl groups. Similar vibration peaks were observed in the spectrum of drug-loaded micelles, viz. 1719.97 cm^{-1}, 1667.24 cm^{-1}, 1420.07 cm^{-1}, 2926.99 cm^{-1}, 1099.20 cm^{-1} and 3478.03 cm^{-1}, respectively (Fig. 5b). The important vibration peaks, characteristics to the pure drug were also observed in the spectrum of drug-loaded micelles with no considerable shifts in their respective wave numbers. Hence, it was stated that there was no chemical interaction between the drug and co-polysaccharide.

4. Conclusion

In this study, a novel amphiphilic gellan co-polysaccharide was designed using C_{18} carbon chain of sorbitan monooleate as lipophilic moiety *via* simple chemical procedure. The co-polysaccharide could form nanomicellar structures in water and entrap budesonide more efficiently. The polysaccharide-based micellar system was devoid of aggregation in aqueous medium and emptied only half of their payload in SNF in 6 h. No chemical interaction was involved in the event of drug release from the interiors of micellar structures. Thus, the prolonged drug release potential of budesonide micellar system in nasal fluids could avoid repetitive application of conventional nasal drops/sprays and afford relief to the patients from the symptoms of allergic rhinitis.

Conflict of interest

The authors report no conflict of interest.

Acknowledgement

The authors convey their sincere thanks to all the management members of Trinity Trust, Gupta College of Technological Sciences, Asansol, West Bengal, India for their kind cooperation in successful completion of this research work.

References

[1] D. Thompson, M.V. Chaubal, Drug Deliv. Technol. 2 (2000) 34–38.
[2] V.P. Torchilin, Cell Mol. Life Sci. 61 (2004) 2549–2559.
[3] S.B. Bhise, A.V. Yadav, A.M. Avachat, R. Malayandi, Asian J. Pharm. 2 (2008) 201–215.
[4] S.H. Yalkowsky, T.J. Roseman, in: S.H. Yalkowsky (Ed.), Techniques of Solubilization of Drugs, Marcel Dekker, New York, 1981, pp. 91–134.
[5] R. Ray, A.H. Kibbe, R. Rowe, P. Shleskey, P. Weller, Handbook of Pharmaceutical Excipients, fourth ed., APhA Publications, Washington DC, 2003.
[6] M.J. Rosen, Surfactants and Interfacial Phenomena, second ed., Wiley Interscience, New York, 1989.
[7] P.G. Djupesland, Drug Deliv. Transl. Res. 3 (2013) 42–62.
[8] R.J. Salib, P.H. Howarth, Drug Safe 26 (2003) 863–893.
[9] J.R. May, P.H. Smith, in: J.T. Dipiro, R.L. Talbert, G.C. Yee, G. Matzke, B. Wells, L.M. Posey (Eds.), Pharmacotherapy: A Pathophysiologic Approach, McGraw-Hill, New York, 2008, pp. 1565–1575.
[10] D.K. Sur, S. Scandale, Am. Fam. Physician 81 (2010) 1440–1446.
[11] N. Nishiyama, K. Kataoka, Pharmacol. Ther. 112 (2006) 630–648.
[12] A.N. Lukyanov, V.P. Torchilin, Adv. Drug Deliv. Rev. 56 (2004) 1273–1289.
[13] D.W. Miller, E.V. Batrakova, T.O. Waltner, A.V. Yu, A.V. Kabanov, Bioconj. Chem. 8 (1997) 649–657.
[14] V.S. Trubetskoy, G.S. Gazelle, G.L. Wolf, V.P. Torchilin, J. Drug Target 4 (1997) 381–388.
[15] M. Yokoyama, M. Miyauchi, N. Yamada, T. Okano, Y. Sakurai, K. Kataoka, S. Inoue, Cancer Res. 50 (1990) 1693–1700.
[16] S.Y. Kim, I.G. Shin, Y.M. Lee, C.G. Cho, Y.K. Sung, J. Control Rel. 51 (1998) 13–22.
[17] S.A. Hagan, A.G.A. Coombes, M.C. Garnett, S.E. Dunn, M.C. Davies, L. Illum, S.S. Davis, S.E. Harding, S. Purkiss, P.R. Gellert, Langmuir 12 (1996) 2153–2161.
[18] A.K. Andrianov, L.G. Payne, Adv. Drug Deliv. Rev. 34 (1998) 155–170.
[19] M.F. Francis, M. Cristea, F.M. Winnik, Pure Appl. Chem. 76 (2004) 1321–1335.
[20] G.-B. Jiang, D. Quan, K. Liao, H. Wang, Mol. Pharm. 3 (2006) 152–160.
[21] G.M. Mekhail, A.O. Kamel, G.A. Awad, N.D. Mortada, Int. J. Biol. Macromol. 51 (2012) 351–363.
[22] Y.-I.I. Jeong, D.-H. Seo, D.-G. Kim, C. Choi, M.-K. Jang, J.-W. Nah, Y. Park, Macromol. Res. 17 (2009) 538–543.
[23] Y. Izumi, N. Kikuta, K. Sakai, H. Takezawa, Carbohydr. Polym. 30 (1996) 121–127.
[24] S.R. Sudhamani, M.S. Prasad, S.K. Udaya, Food Hydrocoll. 17 (2003) 245–250.
[25] W. Kemp, Organic Spectroscopy, third ed., MacMillan Press Ltd., London, 1991.
[26] M. Nidhin, R. Indumathy, K.J. Sreeram, U. Balachandran, Bull. Mater. Sci. 31 (2008) 93–96.
[27] M.P. Bajgai, S. Aryal, D.R. Lee, S.-J. Park, H.Y. Kim, Colloid Polym. Sci. 286 (2008) 517–524.
[28] M.F. Francis, M. Cristea, Y. Yang, F.M. Winnik, Pharm. Res. 22 (2005) 209–219.
[29] X. Li, J. You, F. Cui, Y. Du, H. Yuan, F. Hu, Asian J. Pharm. Sci. 3 (2008) 80–87.
[30] L. Mu, S.S. Feng, J. Control Rel. 76 (2001) 239–254.
[31] T.M. Martin, N. Bandi, R. Shulz, C.B. Roberts, AAPS PharmSciTech 3 (2002) 1–11.
[32] K.K. Gill, S. Nazzal, A. Kaddoumi, Eur. J. Pharm. Biopharm. 79 (2011) 276–284.
[33] K.A. Khan, J. Pharm. Pharmacol. 27 (1975) 48–49.
[34] P. Costa, J.M.S. Lobo, Euro. J. Pharm. Sci. 13 (2001) 123–133.
[35] D.O. Corrigan, A.M. Healy, O.I. Corrigan, Eur. J. Pharm. Biopharm. 62 (2006) 295–305.
[36] R.W. Korsmeyer, R. Gurny, E. Doelker, P. Buri, N.A. Peppas, Int. J. Pharm. 15 (1983) 25–35.
[37] R. Cortesi, L. Ravani, E. Menegatti, E. Esposito, F. Ronconi, Indian J. Pharm. Sci. 5 (2012) 415–421.
[38] J.J. Parmar, D.J. Singh, D.D. Hegde, A.A. Lohade, P.S. Soni, A. Samad, M.D. Menon, Indian J. Pharm. Sci. 72 (2010) 442–448.
[39] M.N. Sahib, Y. Darwis, K.K. Peh, S.A. Abdulameer, Y.T. Tan, Int. J. Nanomedicine 6 (2011) 2351–2366.
[40] M.K. Raval, R.V. Ramani, N.R. Sheth, Int. J. Pharm. Invest. 3 (2013) 203–211.